The Tire as an Intelligent Sensor

Sinem Coleri Ergen, *Member, IEEE*, Alberto Sangiovanni-Vincentelli, *Fellow, IEEE*, Xuening Sun, *Member, IEEE*, Riccardo Tebano, Sayf Alalusi, Giorgio Audisio, and Marco Sabatini

***Abstract*—Active safety systems are based upon the accurate and fast estimation of the value of important dynamical variables such as forces, load transfer, actual tire–road friction (kinetic friction) μ_k, and maximum tire–road friction available (potential friction) μ_p. Measuring these parameters directly from tires offers the potential for improving significantly the performance of active safety systems. We present a distributed architecture for a data-acquisition system that is based on a number of complex intelligent sensors *inside the tire* that form a wireless sensor network with coordination nodes placed on the body of the car. The design of this system has been extremely challenging due to the very limited available energy combined with strict application requirements for data rate, delay, size, weight, and reliability in a highly dynamical environment. Moreover, it required expertise in multiple engineering disciplines, including control-system design, signal processing, integrated-circuit design, communications, real-time software design, antenna design, energy scavenging, and system assembly.**

***Index Terms*—Automotive safety, energy efficiency, energy scavenging, heterogeneous systems, intelligent systems, platform-based design, tires, ultrawideband, wireless sensors.**

I. INTRODUCTION

THE ELECTRONICS industry ecosystem is undergoing a radical change driven by an emerging three-layered architecture characterized by the following features:

1) computing and communication infrastructure that will offer increasingly faster data transfer and manipulation via powerful data centers, compute farms, and wired interconnection;
2) access devices such as PDAs, cell phones, and laptops that allow leveraging of the immense capabilities of the infrastructure for users, which can be humans or any of the intelligent physical systems as follows;
3) a swarm of sensors, actuators, and local computing capabilities immersed in all kinds of physical systems that offer a wide variety of personal or broad-use services, e.g., a mechanical system such as an automobile, a train, or a plane; an electrical system such as an electrical motor or generator; a chemical system such as a distillation plant; health-care equipment such as a pacemaker; a distributed environment monitoring and control system or a security system for access control to protected areas.

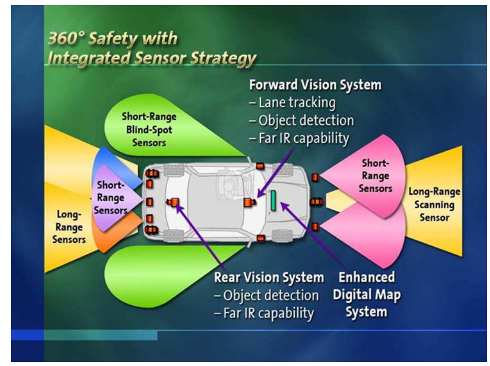

Fig. 1. 360° integrated safety.

In particular, this evolution will have a dramatic effect on automobiles, particularly when considering safety. Road-traffic injuries still represent about 25% of worldwide injury-related deaths (the leading cause) with an estimated 1.2 million deaths (2004) each year [9]. Passive safety devices, such as crumple zones, seat belts, and airbags, work passively to prevent injuries and are standards today. Obviously, these devices, albeit effective, are nowhere near to *preventing accidents*. Active safety is the frontier for original equipment manufacturers and suppliers to eliminate deadly accidents. Active safety systems use information about the external environment of a vehicle to change its behavior in precrash time period or during the crash event, with the ultimate goal of avoiding a crash altogether. The *zero-accident car* includes both autonomous systems, such as radar-based crash-avoidance systems, and cooperative systems that rely on vehicle-to-vehicle and vehicle-to-infrastructure (and vice versa) communication. Eventually, we believe autonomous driving will be possible based on wireless and wired networks of powerful sensors (see Fig. 1, courtesy of General Motors) and complex control algorithms implemented on a distributed computing platform. In fact, research efforts into autonomous accident-free vehicles began in the 1980s with the EUREKA Prometheus project [7].

Early work on active safety systems were primarily focused on improving the longitudinal motion dynamics, particularly on more effective antilock braking systems and traction-control (TC) systems. TC systems prevent the wheel from slipping while improving vehicle stability and control by maximizing the tractive and lateral forces between the vehicle's tire and

Manuscript received July 14, 2008; revised November 13, 2008. Current version published June 17, 2009. This work was supported in part by the Gigascale System Research Center, by the MICRO program of the State of California, and by the Artist Design Network of Excellence. This paper was recommended by Associate Editor M. Di Natale.

S. C. Ergen is with the Pirelli/Telecom Italia, Wireless Sensor Networks Berkeley Laboratory, Berkeley, CA 94704 USA.

A. Sangiovanni-Vincentelli and X. Sun are with the Department of Electrical Engineering and Computer Science, University of California, Berkeley, Berkeley, CA 94720-1500 USA (e-mail: alberto@eecs.berkeley.edu).

R. Tebano, G. Audisio, and M. Sabatini are with Pirelli Tyres S.p.A., 20126 Milano, Italy (e-mail: riccardo.tebano@pirelli.com).

S. Alalusi was with the Pirelli/Telecom Italia, Wireless Sensor Networks Berkeley Laboratory, Berkeley, CA 94704 USA. He is now with TransRobotics, San Francisco Bay Area, Hayward, CA 94545 USA.

Color versions of one or more of the figures in this paper are available online at http://ieeexplore.ieee.org.

Digital Object Identifier 10.1109/TCAD.2009.2022879

the road. This was followed by more powerful vehicle-stability control (VSC) systems, e.g., electronic stability program, VSC, and dynamic stability control. These systems use both brakes and engine torque to stabilize the vehicle in extreme handling situations by controlling the yaw motion. Active suspension systems are also an important part in active safety systems. They have been traditionally designed by trading-off three conflicting criteria: road holding, load carrying, and passenger comfort. The suspension system must support the vehicle, provide directional control during handling maneuvers, and provide effective isolation of passengers/payload from road disturbances.

The active safety control systems described earlier are based upon the estimation of vehicle dynamics variables such as forces, load transfer, actual tire–road friction (kinetic friction) μ_k, and maximum tire–road friction available (potential friction) μ_p, which is probably the most important parameter for the improvement of vehicle dynamic control systems [10]. The more accurate and "real time" the parameter estimation is, the better the overall performance of the control system. Currently, most of these variables are indirectly estimated using onboard sensors. With a more accurate estimation, we could even identify road-surface condition in real time. By detecting the change in the slope of the friction versus slip curve, regions of slippery surface can be identified [10], [11].

The Apollo project [1] attempted to gain real-time information by using the tire as a sensor. However, until recent developments in low-power wireless communication and energy scavenging, this approach was expensive and remained mostly in the research domain, since it was not easily adoptable as a consumer product. Currently, state-of-the-art tire monitoring systems [2]–[6] primarily acquire low-duty cycle data such as tire pressure, temperature, and/or material strain of the tire. However, they are not equipped to sense and transmit high-speed dynamic variables used for real-time active safety control systems.

In this paper, we describe the considerations, tradeoffs, and decisions used to design a real-time system for *extracting directly from the tire* relevant information to improve significantly active safety control systems and enable the development of a wide range of new applications. Placing a sensor system that could compute the quantities of interest in a tire and transmit this information to a safety controller is a very challenging proposition for technical, reliability, and economic reasons.

In particular, the major challenges to face are as follows.

1) The inside of a tire is a harsh environment with high accelerations (at 200 km/h, we have an acceleration equal to 3000 g's inside the inner liner) and cannot be reached without taking the tire off the wheel. This situation poses very difficult problems: The high centrifugal acceleration implies that the sensor be lightweight, robust, and small; the fact that the tire moves continuously with respect to the body of the car forces us to choose a wireless-communication link.
2) Among the available miniaturized sensors, accelerometers were chosen for our application, since they exhibit a number of advantages: They are well understood, widely available, reliable, accurate, and relatively inexpensive. However, devising algorithms that could compute the quantities of interest from accelerometer data is nontrivial [8].
3) Since accelerometer data have to be generated/delivered at each revolution of the tire, the data-rate requirement could quickly deplete any battery that meet the weight and size requirements. Replacing batteries is obviously out of the question because of the difficulty of reaching inside the tire. Hence, some sort of energy scavenging is needed that relies on a transducer of mechanical energy into electrical energy via inductive or capacitive coupling or on illuminator technologies based on transferring electromagnetic power to a remote device via an RF link. These approaches, however, can only provide energy of less than 1 $\mathrm{mW/cm^2}$, thus limiting the total energy available for sensing, computing, transmission, and reception.
4) The radio link from the tires to the onboard controllers must be sustainable with limited energy and resilient to the harsh tire environment.
5) The communication protocol between the various elements of the system has to be carefully designed to use the minimum amount of power while making sure that data reach the destination reliably and on time.

In this paper, we describe the analysis and decision processes followed to design a wireless sensing subsystem based on intelligent sensor nodes that are inside the tire and that solve the challenges described earlier. The final phase of the design has not been completed as yet; we are still evaluating and prototyping the energy-scavenging and wireless-communication subsystems. In Section II, we present how to extract the information of interest for safety control from accelerometers. In Section III, we introduce the overall architecture of the system. Then, in Section IV, we discuss the architecture of the intelligent sensor node and describe its components. In the following sections, we present the most interesting and novel aspects of the design that refer to the communication scheme: An ultrawideband (UWB) radio designed specifically for this application (Section V) and a new medium-access-control (MAC) protocol called implicit-scheduled time-divided MAC (ISTD-MAC) (Section VI). In Section VII, we introduce the methodology followed in the design. In Section VIII, we draw conclusions, and we chart the road for the future full-fledged implementation of the Intelligent Tire Acquisition system.

II. Extracting Variables of Interest From Accelerometers

The information necessary to significantly improve active safety and active dynamics control systems is extracted using data-processing algorithms operating at two distinct levels as follows.

1) *Tire Level*. They range from simple temperature and pressure information extraction to load, lateral, and longitudinal forces and potential friction estimation based upon more complex accelerometer data processing and modeling. Tire wear and aquaplaning are also extracted with algorithms at the tire level.
2) *Vehicle Level*. They range from load distribution and dynamic load-transfer estimation to amount of friction available.

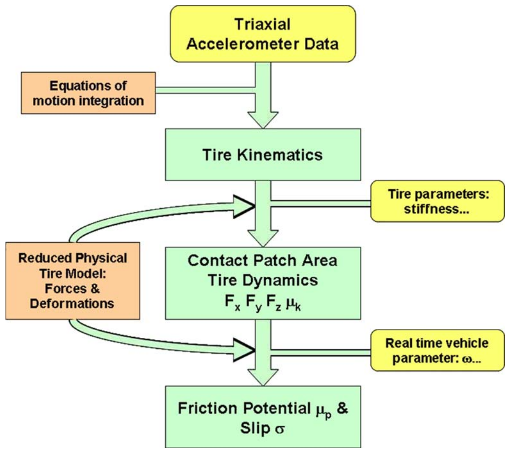

Fig. 2. Algorithm structure.

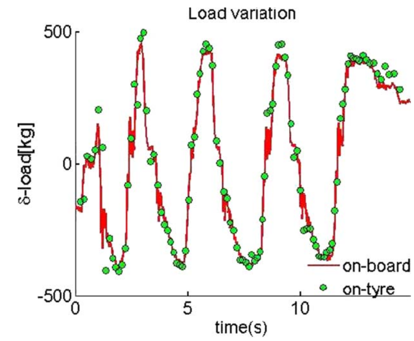

Fig. 3. Load transfer during multiple acceleration–deceleration maneuvers. Circles represent the estimated load transfer with the Intelligent Tire system while the solid line is the traditional load-estimation method based upon sensors on vehicle.

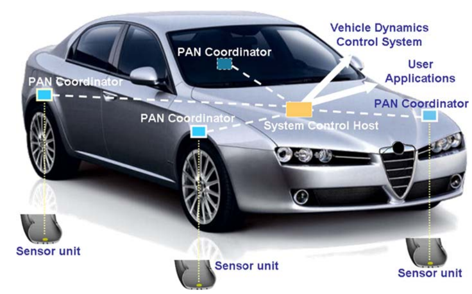

Fig. 4. System architecture.

This section gives an overview of how relevant data at these two levels are obtained from raw sensor data.

In Fig. 2, we show the method proposed to estimate forces and kinetic friction, F_x, F_y, F_z, and μ_k along with other important tire–road dynamic interaction parameters, i.e., potential friction μ_p and tire slip σ, using the measurements provided by the accelerometers in the sensor nodes. The key aspect of the extraction method is the analysis of the dynamics of the contact patch area of the tire. This dynamics contains specific information about the variables earlier.

The first stage derives the tire kinematics by solving the corresponding equations of motion, i.e., by double integration of accelerations as measured by the accelerometers and with proper boundary conditions. From this and some key tire parameters, we obtain the "experimental" dynamics in the patch area, i.e., the area of the tire that is in contact with the ground from which we can obtain the forces of interest.

To obtain the other important parameters such as the potential friction, we need a fairly complex path as described in the figure. To do so, we developed an ad hoc tire physical model that includes parameters that are typical of the particular tire considered and of the dynamical condition of the car. At this second stage, the dynamics of the contact-patch-area tire deformations are obtained using a theoretical tire force–deformation frame. The potential friction is a parameter for the calculation of the deformations of the patch area.

The last stage identifies the correct value of the theoretical model parameters (e.g., μ_k) by "fitting" them so that the results of the theoretical model "match" the ones obtained by measurements. This is done by finding the values of the parameters so that an appropriate metric defined to evaluate the "difference" between the output of the theoretical model and the measured results is minimized as is customary in identification problems. There are, of course, several metrics that can be used to measure the difference of the outputs: For example, the minimum of the maximum difference over the set of experiments or the sum of the squares of the differences at every point of the test set. The metrics to be used is a compromise between the computational burden and the accuracy of the final result. In preliminary experiments, we obtain an error in the important parameters on the order of 5%.

The data collected by the Intelligent Tire can be used in multiple ways. An example of the information that can be collected is the computation of the vehicle load transfer in nonstationary dynamic maneuvers consisting of multiple acceleration and deceleration sequences. Fig. 3 shows the load-transfer estimation obtained with the Intelligent Tire system versus the conventional load-estimation method based upon sensors located on the vehicle. In addition, the Intelligent Tire Acquisition system allows the distinguishing of single-tire load behavior.

III. System Architecture

Fig. 4 shows the architecture of the tire sensor network. The main components of the system are organized in a hierarchical manner in a personal area network (PAN) defined as a collection of cooperating devices, which are associated and share the same address space. At the lowest level, sensor nodes, located inside the tires, are responsible for data acquisition, processing, and transmission to the in-vehicle equipment. Placing more than one sensor inside each tire achieves increased accuracy and reliability of the measurements performed. For example, three sensor devices may be located at an angle of 120° with respect to each other. This configuration allows improved knowledge of spatial variation of tire/road interaction parameters, albeit the availability to the vehicle dynamics control system of this "knowledge" is subject to a time delay of half a wheel turn, independent of the number of sensor nodes inside the tire.

The *PAN coordinator* at the upper level of the hierarchy is mounted in the vehicle and powered by the vehicle main. It manages the communication with the sensor nodes in the same tire, receives data from them, and is the master of synchronization. PAN coordinators can be connected to each other via a wired network or even a vehicle system bus such as CAN and FlexRay. The highest layer of the network is the *System Control*

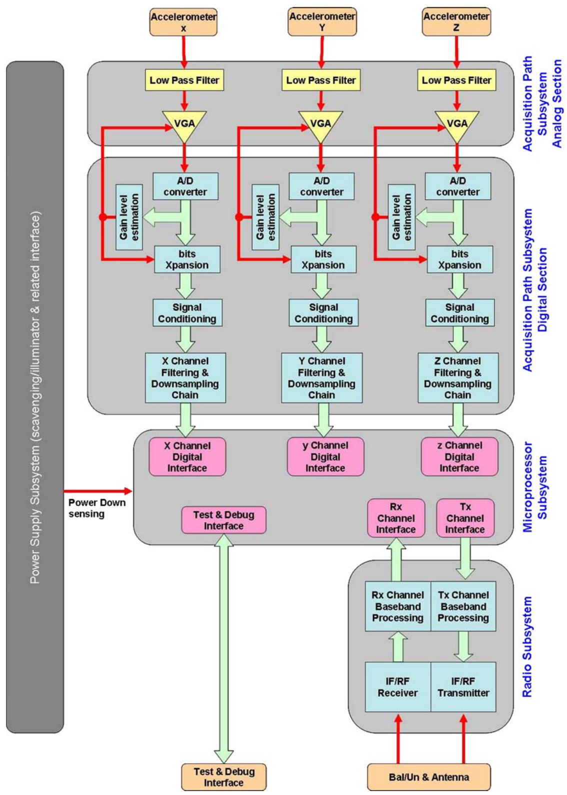

Fig. 5. Sensor-node architecture.

Host. This device is responsible for coordinating all PAN coordinators, interfacing them with the vehicle main control and providing a bridge to the vehicle system bus. The System Control Host is responsible for transferring commands to the sensor nodes from the vehicle main control and information acquired by the PAN coordinators to the vehicle main control via the vehicle system bus. The System Control Host may be implemented as one of the PAN coordinators, having enhanced functions with respect to other coordinators.

The resulting network architecture has a cluster-tree structure. We chose to have one PAN coordinator corresponding to each tire instead of a common coordinator, since by doing so, we increase the total throughput by limiting the number of sensors controlled by each coordinator, and we minimize the distance between sensor nodes and PAN coordinator for a more robust communication. A cluster-tree structure is suitable for this application, since sensor nodes need not communicate with each other but only with the PAN coordinator.

IV. Sensor Node

The sensor node (see Fig. 5) is the in-tire device with the tasks of acquiring data from the tire, executing preliminary digital signal processor (DSP) processing on them, such as signal conditioning and compensations, and to send data on the RF link. The most important requirements of the Intelligent Tire are an unlimited lifetime and a small size. The sensor nodes inside the tires should be operational for the lifetime of the tire. Moreover, the technology should satisfy the wide-temperature-range requirements and robustness to high accelerations: Extreme temperatures range from -40 °C in winter up to 100 °C in summer time, and an object mounted on inner lining is subject to a radial acceleration up to 3000 g's at 200 km/h.

The design of each component of the Intelligent Tire is nontrivial but the radio link and the power generation and management system are by far the most challenging. In the following sections, we describe details of each of the components together with the challenges to be considered in system assembly.

A. *Power-Supply Subsystem*

The most common way of providing power to wireless devices is storing chemical energy in a battery. In battery technologies, however, the lifetime of the node will be determined by the fixed amount of energy stored on the device regardless of the form of energy storage. There is no known battery chemistry that can deliver the necessary amount of energy for the volume available. Furthermore, the accelerations involved and the high-temperature requirements make battery technology unfeasible for this application.

Since energy storage in the nodes is impossible, alternative methods of providing power fall into one of two categories.

1) Scavenging available power at the node [28]. The most suitable technology for the tire system relies on scavenging power from vibrations. Devices include electromagnetic, electrostatic, and piezoelectric methods to convert mechanical motion into electricity. The amount of power generated by the scavenger depends on the technology chosen, on the size of the scavenger, and on the environmental conditions such as vibrations, elongation stresses, and temperature gradients. These approaches provide energy levels in 10–200-μW range for real-world tire scenarios. It is conceivable that, due to strong market demands, progress will be made in terms of power output.
2) Electromagnetic coupling. The possible methods of providing electromagnetic wireless power transfer include magnetic field coupling via inductive action between two coils, magnetic field coupling via self-resonant coils, and microwave radiation beam via highly directive antennas. An illuminator is a main-powered antenna transferring electromagnetic power to a remote device via an RF link. Power is collected by the remote device by means of a suitable receiving antenna. This technique is used for RFID applications. In our case, the illuminator would have to be placed on the wheel as well so that the amount of energy delivered is optimized.

We are currently investigating both possibilities. Other means of transferring power to the nodes such as acoustic emitters and lasers are not suitable for tire systems due to poor transmission through the tire.

Both alternatives provide a time-dependent power, since power generation and coupling is strictly related to the wheel motion and position. Therefore, raw generated power must be conditioned to provide a power supply that is almost constant, at least within a complete wheel rotation. It is important to consider that, during normal operating conditions, the wheel may stop its motion and power cannot be supplied any longer: For this reason, a power sensing function has to be implemented, such that the microcontroller is informed as soon as power supplied becomes insufficient. In this situation, the node goes into a power-down mode in a controlled and "safe" manner. The power sensing function determines the start of communication in MAC protocol design, as we will see in Section VI. Furthermore, the ultra-low power-consumption constraint suggests that acquisition, reception, and transmission phases are kept separated as much as possible to spread power consumption on each wheel round and avoid high consumption peaks caused by overlapping different activities. This places timing constraints on the sensing and communication functions.

B. Sensor- and Acquisition-Path Subsystems

The sensor is a triaxial accelerometer, mounted inside the tire on top of the inner liner, oriented so that the three axes measure signals in the radial, circumferential (tangential), and lateral directions with respect to the tire circumference. Therefore, the input flow to the sensor node consists of three data streams. The requirements that drive the choice of technology for the accelerometers are reliability and reproducibility, accuracy and resolution, power consumption, size, and cost.

Few available technologies fit all of the requirements listed above. Stringent power requirements exclude the use of piezoresistive technology. Today's accelerometers based on piezoresistive technology have power consumptions in the range of several milliwatts. Even though we may consider a custom-built product that could consume up to a few hundred microwatts, this technology intrinsically requires a bias so it will always be more power hungry than capacitive or piezoelectric devices.

The two main piezoelectric non-microelectromechanical-system (MEMS)-based technologies are crystal and ceramic based. The latter is somewhat smaller given the same g sensitivity, although less stable in temperature, and with higher process sensitivity spread. This technology is capable of providing the dynamic range of interest, with reliability indexes suitable for our application, and it is intrinsically very low power, providing a charge as an input to the acquisition path satisfying the no-bias-current requirements. However, it is fairly large so it does not fit our size requirement.

Current MEMS-based technologies include the following examples:

1) piezoelectric technology consisting of deposition of a thin piezoelectric film of lead titanate onto a MEMS silicon structure;
2) piezoresistive technology consisting of etching semiconducting silicon gauges;
3) capacitive technology.

The capacitive technology is the technology of choice, since it is used in airbags with millions of devices shipped annually, having reached a reliability standard that complies with the demanding requirements of our tire application. It is also very low cost when manufactured in volume and fits the size constraints. The challenge to deploy this technology is to compensate for an intrinsic spread of process parameters and high dependences of key design parameters such as sensitivity (millivolts or picocoulombs per g) and offset to temperature and manufacturing process. The challenge of extracting a wide dynamic range with the required resolution is responsibility of the circuitry that interfaces the MEMS device. The accelerometers themselves are simple devices; all compensations and corrections to the sampled signals are provided by the other components of the sensor node. The acquisition path is responsible for the transformation of the signal acquired by the accelerometers into digital signals, as shown in Fig. 5. The acquisition path provides an analog section and a digital section.

1) The analog section amplifies and filters the acquired signal. Then, analog data are converted and passed to a digital section. Oversampling techniques may be used; thus, signals may be acquired at sampling frequencies higher than their final sampling rate.
2) The digital section is responsible for signal conditioning for correcting accelerometer imperfections such as offset bias and resonant-frequency compensation. Data are sent to a processing chain that provides filtering and decimation to the final sampling rate. Automatic-gain-control techniques may be used to keep the SNR constant, even at low levels of signal dynamics.

C. Microprocessor Subsystem

A single-core DSP is responsible to manage the communication protocol; all the functions that control the activity of the sensor nodes, such as command execution, system monitoring, and diagnostics; and the following typical DSP functions:

1) estimation and compensation of signal nonlinearity;
2) estimation and compensation of crosstalk among the different accelerometers;
3) estimation of bias and offset;
4) data compression for reducing the input throughput;
5) algorithms required by the communication protocol.

Note that some of these algorithms may be implemented by specialized HW devices to reduce power consumption and increase performance if product testing will uncover problems in these areas.

D. Radio Subsystem

The radio subsystem is responsible for the following functions:

1) transforming digital data to be sent to the PAN coordinator into analog signals modulated over the desired transmission channel;
2) receiving analog data from the transmission channel and transforming them into baseband digital data.

The radio subsystem consists of an SW driver and an HW transceiver. The transceiver implements the physical-layer components, related to channel coding/decoding, modulation and conversions between analog signals to/from digital data, synchronization, and generation of events on a fine-grain timescale (bit or chip level). The SW driver implements the MAC layer and higher network layer components and manages all events and synchronization requirements at a coarse-grain timescale (frame level). Amplifiers are included in the radio channel to increase the power of the signal before transmission or before processing the received signals. This subsystem is expected to give significant contribution to the overall power-consumption budget together with the acquisition chain, and for this reason, its design is of paramount importance. We dedicate the next section to a detailed description of the solutions adopted.

E. System Assembly

The operating conditions of the sensor nodes place hard constraints on the weight and size of each unit. First, the mass of the sensors must be kept minimal so that it does not affect the tire characteristics and the accelerometer signals. In addition, since the nodes are to be mounted into the rubber of the tire body, its size must be small (around 1 cm^3) so that extra mechanical devices do not need to be added to the system package for mounting. The small-size requirement directly competes with requirements needed for the antenna and energy scavenger, where increased size and mass allow better performance. These competing constraints create many challenges for system optimization. Furthermore, the high temperature, centrifugal forces, and mechanical stresses that the system must withstand are nontrivial tasks for system assembly.

V. Radio Subsystem

The communication environment in the Intelligent Tire system is very harsh. For the uplink transmission, UWB transmission is preferred to narrowband transmission and spread-spectrum techniques due the presence of severe multipath and lack of line-of-sight (LOS) [22]. In addition to being robust to intersymbol interference due to multipath fading, the UWB systems hide signals below the noise floor causing little or no interference to existing systems and mitigate the performance degradation due to narrowband interference. We specifically utilize impulse-based UWB technology due to the simple transmitter architecture, which makes it ideal for the low-power high-data-rate uplink transmission from sensor node to vehicle. The main drawback is that UWB receiver design is challenging due to the sensitivity requirements. A low data rate is required for the downlink, so we use narrowband transmission and an ultra-low-power receiver on the sensor nodes.

A. Uplink Communication

UWB technology has emerged in recent years as the ideal solution for low-cost low-power short-range wireless data transmission. FCC defines UWB as any radio technology for which the emitted signal bandwidth exceeds the lesser of 500 MHz and 20% of the center frequency [15]. In 2002, FCC has allocated the 3.1–10.6-GHz band for the unlicensed use of UWB applications; however, these systems must limit energy emission to follow the FCC spectral mask [16] so that no interference is caused to existing technologies in the band.

To design the UWB system, it is necessary to understand the transmission channel that operates on the transmitted signal. There have been studies of typical channels for UWB communication systems in indoor and outdoor scenarios. However, these environments are much larger than the wavelengths present in the signal, and they are mostly empty. In contrast, the area around the tire is quite different. There are two large reflectors in the immediate vicinity of the node: the wheel rim and the wheel arch of the car's body. Both of these are virtually always metal and are curved such that they tend to reflect incident waves back into the area, confining them. In addition, the node is inside the tire and must transmit through the tire in some way: A true LOS channel is impossible, since the tire, composed of a metal mesh and rubber, attenuates the signal dramatically.

Fig. 6. Channel measurement setup.

For the channel measurements, a wrecked Hyundai Accent was purchased, and the right rear quarter of the car was cut off. The wheel arch and all machinery inside including the suspension were preserved. The SkyCross UWB antennas are placed inside the tire under the tire tread and at the highest point inside the wheel arch. To generate the transmit signal, a pulse generator is used. It is capable of pulses with 100-ps width. To receive the signal, the receive antenna is connected to a pulse amplifier through a short cable. The amplified signal is then sent to a 20-GS/s 6-GHz input bandwidth oscilloscope. The setup in the Berkeley Wireless Research Center is shown in Fig. 6.

The channel impulse response is based on the modified Saleh–Valenzuela (SV) model developed for UWB systems [12]. The model consists of clusters that arrive according to a Poisson process. The power envelope for the clusters follows an exponential-decay random process. Each cluster is made up of rays which also arrive according to a Poisson process and decay according to an exponential random process.

An initial comparison with the measured data showed that the SV model matched quite closely once the parameters are set correctly. The only problem was that there was too much incoming energy at very early times due to the exponential envelope. Intuitively, this early time energy is due to a strong LOS or at least significant energy traveling in a geometrically straight line from the transmitter to the receiver. In the case of the tire channel, the LOS is probably through the tire thread and, therefore, is very weak. The strongest rays travel through the sidewalls and experience at least one reflection before arriving at the receiver. Thus, the exponential random envelope for the cluster arrivals was deemed inappropriate. The base SV model was modified slightly. The exponential envelope for the cluster power was changed to a Rayleigh random envelope. The Rayleigh distribution has maximum energy at some time greater than zero but usually a small number. In our case, that is a few nanoseconds. All other aspects of the model were unchanged: Poisson process for cluster and ray arrival times and exponential decay of ray power within a cluster. This new model is referred to as the SV-R model. An instance of the resulting model is shown in Fig. 7.

The experiments are performed for two tires, Hankook 175/70R13 and Pirelli Pzero Nero M+S 204/45R16, at 8 positions around the rotation of the tire, i.e., every 45°. The arrival-time process for the clusters is governed primarily by λ_c, whereas the ray-arrival-time process is governed by the parameter λ_r. Typical values for λ_c are slightly less than 10 ns, and λ_r is typically a few nanoseconds. These values are significantly lower than the scenarios found in the 802.15.4a standard. This

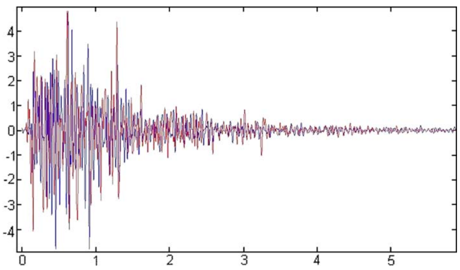

Fig. 7. (Red) Impulse response of SV-R model compared to (blue) measured data. The x-axis is in 10 ns.

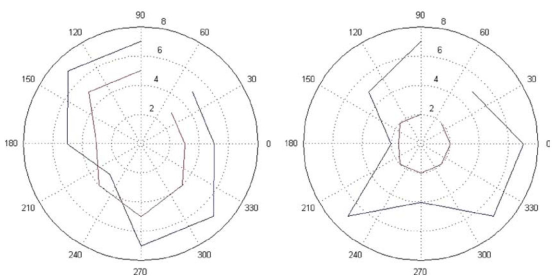

Fig. 8. (Outer, blue) γ_c and (inner, red) γ_r for (left) Hankook and (right) Pirelli in nanoseconds.

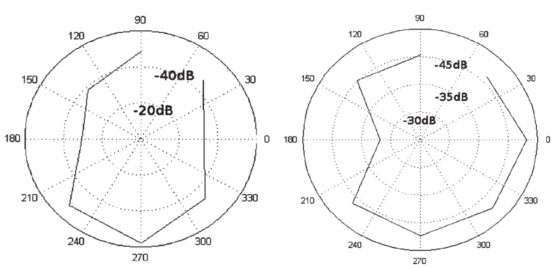

Fig. 9. α for (left) Hankook and (right) Pirelli.

is due to the much shorter flight distances involved in the tire area as compared to the scenarios considered in the standard. λ_c and λ_r were found not to vary much in different positions. Much greater variation was observed for cluster decaying factor and ray decaying factor, γ_c and γ_r, respectively. They are shown in Fig. 8.

A very important system parameter that can be extracted from the time-domain model is the delay spread. Delay spread is defined as the time at which the impulse response falls below the noise floor. In the measurements, the noise floor is very low, and the delay spread is 20–30 ns, as shown, for example, in Fig. 7. The final major parameter that was extracted was the channel attenuation, and it is designated as α, as shown in Fig. 9. The values for the Pirelli tire are generally larger than for the Hankook tire. This is easily attributed to the thicker and more robust construction of the Pirelli tire. Following the determination of channel model, the UWB system is designed.

There are two broad categories of UWB systems: impulse radios (IRs) and multiband orthogonal frequency-division multiplexing (MB-OFDM) radios. IR systems directly generate the UWB frequency spectrum via ultrashort pulses, whereas MB-OFDM is an adaptation of traditional narrowband OFDM technology that forms an aggregate equivalent bandwidth of at least 500 MHz. We focus on IR, since the energy-constrained environment of the application is unable to handle the architectural complexity of the MB-OFDM systems.

1) Pulse Shape: Any pulse shape can be used for UWB systems as long as the frequency response satisfies FCC requirements. The most common pulse shapes for IRs in literature are Gaussian pulses and its derivatives [14].

The frequency spectrums of these pulses are well behaved as compared to other pulse shapes, making them ideal for UWB applications. However, these pulses are quite difficult to generate or control, usually requiring a sophisticated transmission-line-based design. The center frequency of a Gaussian pulse is also hard to control, since even the slightest change in pulse shape, on the order of picoseconds, can shift the center frequency by hundreds of megahertz. In addition, generating Gaussian pulse that fit in the FCC spectrum mask is also not a trivial task. Most likely, some kind of filter is needed for the pulse, which increases transmitter complexity. As a result, Gaussian pulses are mainly suited for applications in the 0–1-GHz band.

The other two common pulse shapes are rectangular and triangular sinusoids, which are directly adapted from narrowband-radio design concepts. In this paper, the main pulse is first generated whose frequency response fits in the baseband equivalent of the FCC mask. The pulse is then upconverted to the desired carrier frequency with a carrier pulse. The benefit is that the pulse shapes are straightforward to generate without any special filters or hardware, and the center frequency is easy to control. The triangular sinusoid is a better fit in the FCC mask and offers more bandwidth in the main lobe of the frequency response. Thus, the triangular sinusoidal pulse is the natural choice.

2) Modulation: Only binary-modulation schemes were explored for the Intelligent Tire system, since complex modulations would also increase power consumption due to more complex architectures. Specifically, pulse-amplitude modulation (PAM), on–off keying (OOK), pulse-position modulation (PPM), and binary phase-shift keying (BPSK) are compared.

In PAM and OOK, the “0” and “1” bits are represented by analog signals of two distinct peak amplitudes. Specifically, OOK only outputs a pulse for the “1” bit. The advantage is that it is relatively straightforward to implement, without adding any additional components to the transmitter. The disadvantage is that if the difference between the amplitudes for the “0” bit signal and the “1” bit signal is too small, then the signal is extremely sensitive to channel noise and interference. In addition, in OOK, a “0” bit cannot be distinguished from the lack of a signal at the receiver, making timing recovery and synchronization more difficult.

For PPM, information is conveyed via the position of a pulse in the time domain with respect to a specific location. PPM is more robust to channel noise than most PAM systems. The bit-detection process is simple; however, it requires careful synchronization between the transmitter and the receiver, since the locations of the “0” and “1” bits are critical for this modulation scheme. Luckily, UWB signals have a wide delay spread relative to its pulsewidth due to the abundance of multipath components, which helps relax the synchronization requirements. However, synchronization must still be on the order of tens of nanoseconds.

BPSK distinguishes between the “0” and “1” bits by the phase of the signal. A major disadvantage to this scheme is that an energy-detection approach is no longer possible for bit detection, since both the “0” and “1” signal gives the

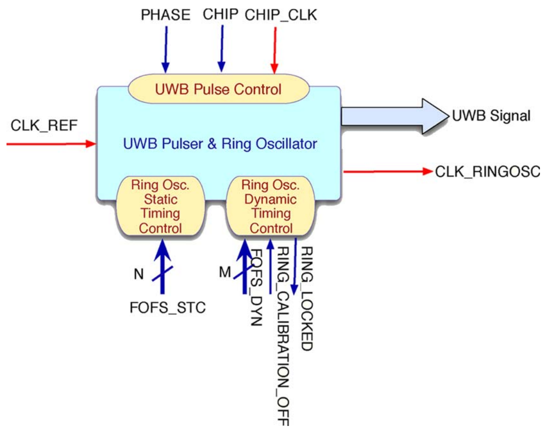

Fig. 10. UWB transmitter.

TABLE I
UWB RECEIVER SCORECARD

	ED - RF	ED - BB	Corr - RF	Corr - BB
SNR	5	4	2	3
Multipath	3	1	4	3
Carr Offset	1	1	3	3
Sync Misalign	2	1	3	2

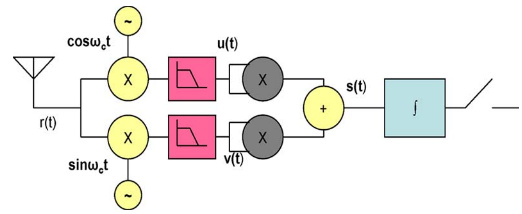

Fig. 11. Energy detection at baseband receiver for UWB detection.

same energy. Instead, coherent receiver architectures, such as a matched-filter design, must be utilized to track the phase of the incoming signals, which complicates receiver architecture, particularly in the presence of an unpredictable channel.

PPM turns out to be the best option for this application due to the simplicity allowed for the receiver architecture and robustness under severe in-band interference and multipath effects. Compared to BPSK, PPM allows the use of noncoherent receiver architectures such as energy-detection receiver since we do not need to track the phase of the incoming signals. Compared to PAM or OOK, PPM is more robust and inherently carries timing information from the sensor nodes allowing better synchronization with the PAN coordinator.

3) UWB Communication Architecture:

Transmitter front end: The uplink radio needs to transmit at a fairly high data rate, greater than 1 Mb/s, and needs to consume as little power as possible in the transmitter. Thus, we chose a simple transmitter architecture consisting of a ring oscillator to generate the carrier signal and a pulse controller to generate the modulated baseband signal, as shown in Fig. 10.

Receiver front end: Power constraints of the sensor nodes allowed us very few options to play with for the transmitter. The receiver on the PAN coordinator, however, was not subject to such stringent constraints; thus, several architecture alternatives were feasible. Since the Intelligent Tire system had such asymmetric design constraints, much of the burden for combating adverse channel effects have been shifted to the receiver side. The goal was to find a receiver architecture that had good enough sensitivity to capture the UWB signals in the presence of a harsh channel. In addition, the receiver needs to be robust to in-band interference signals and maintain a relatively consistent performance. A matched-filter type of design was out of the question, since the short duration of UWB signal would place tremendous burden on the analog-to-digital converters at over 10-GHz sampling frequency. Although the PAN coordinator is not as power constrained as the sensor nodes, it is still limited. The choices that were evaluated were energy-detection receivers at RF and baseband, and correlation receivers at RF and baseband. Scorecard of each of the receiver architectures is shown in Table I. Scores range from 1 to 5, where 5 is the most sensitive, and 1 is the least.

As expected, energy-detection-based receivers are more sensitive to SNR, whereas correlation-based receivers become very unpredictable in the presence of multipath effects. Overall, energy-detection at baseband was determined to be the best detection algorithm to be used as UWB receiver. UWB signals have a very rich multipath profile, which makes correlation-based receivers unreliable to use. Although energy-detection receivers are prone to interferences from other signals, we hope that the rich multipath profile of UWB signals will help to mitigate this problem.

The architecture for the uplink receiver, shown in Fig. 11, is a modification of the classical energy-detection receiver that first downconverts the incoming signal band and performs energy detection. The incoming signal is first split into two paths and downconverted in I and Q channels. The two signals are then filtered to remove unwanted higher order signals. The resulting signals are squared and added to produce the final signal. This signal is an estimate of the power of the modulating signal that is not sensitive to the phase of the incoming signal. The signal is finally integrated, and the output (aka chips) is sampled and made available to the digital baseband section for detection.

Baseband processing: The packet structure and baseband processing of the system are based on, but not necessarily compliant with, IEEE 802.15.4a standard [13] and consist of the following processes.

1) *Chip synchronization*: Using the received preamble, finds the locations of the incoming pulses to synchronize the analog front end in preparation for the incoming packet.
2) *Despreader*: Decodes the incoming chips into bits. In the Intelligent Tire system, an 8-b pseudonoise (PN) sequence spreading is used to combat channel effects.
3) *Packet detection*: Detects the beginning and end of a packet.
4) *Error-correcting-codes (ECC) decoding*: A Reed–Solomon (RS) coding scheme, and a half-rate convolution encoder is used to reduce error.
5) *Cyclic-redundancy-check (CRC)*: Parity check for packet validity.

The transmitter baseband-processing chain contains the corresponding components, which are mapped onto a low-power DSP. The main purpose of the digital baseband blocks in the transmitter is packet generation (Fig. 12). The packet structure used is inspired by the structure specified in IEEE 802.15.4a with a few modifications to suit our application. First, given M information bits from the application, MAC packet is formed by adding MAC header including 1 B for sequence number

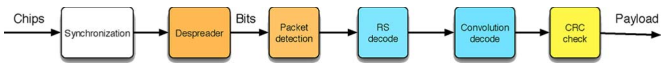

Fig. 12. Receiver-baseband processing.

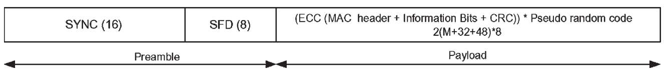

Fig. 13. Packet structure used for the application with respective number of symbols (chips) for each field. We assume $M = 32$ B for the MAC simulations.

to detect packet losses and 2 B for destination and source address, and a CRC calculated over both the MAC header and the data payload for packet validation. The method used was the common CRC-8 procedure. Next, following procedures in the standard, the data are encoded for error correction. The forward error-correction encoder consists of an inner RS encoder and an outer convolutional encoder. The RS encoder appends 48 parity bits to the MAC packet and feeds into a half-rate convolutional encoder, which produces $2(M + 32 + 48)$ b. The RS encoder uses the following generator polynomial:

$$\begin{aligned} g(x) &= \prod_{k=1}^{8}(x + a^k) \\ &= x^8 + 55x^7 + 61x^6 + 37x^5 + 48x^4 \\ &\quad + 47x^3 + 20x^2 + 6x + 22. \end{aligned} \tag{1}$$

Then, spreading is done by directly mapping each symbol to a constant PN sequence. This differs from the standard, which employs a time-hopping spreading technique based on a time-varying PN sequence. The change to direct PN spreading allows reduced complexity in the transmitter of the sensor nodes and less stringent synchronization requirements for the receiver architecture.

The preamble then consists of two fields: SYNC, responsible for establishing clock synchronization and timing recovery, and the start field delimiter (SFD), responsible for denoting the beginning of an incoming packet to the receiver. Due to the time constraint of the transmission frame, we use the smallest preamble size dictated by the standard, i.e., 16 SYNC symbols and 8 SFD symbols, by default but the length can be adjusted by the PAN coordinator if needed. In addition, since the length and the data rate of the packet for our application is fixed, we eliminate the PHY header. The final packet structure used for the Intelligent Tire system is shown in Fig. 13. An additional deviation from the standard's UWB PHY specifications is the modulation scheme used. As mentioned in Section V-A-2, binary PPM (BPM) is used for this application to reduce receiver complexity, whereas the standard uses BPM-BPSK modulation for each two symbols.

UWB simulation: Upon selecting the communication architecture, we need to extract the performance information of the PHY layer into the MAC layer. Since physical implementation is not yet complete, we can only evaluate at the functional level. Specifically, the performance is reported in terms of chip-error rate (CER) in Table II. This is the lowest level of abstraction for the radio before physical implementation. In-band interference for the channel was modeled as an additive white Gaussian noise channel with appropriate SNR assignment. The multipath profile for the channel is based on the channel model we developed. Each result is based on a simulation of 10 000

TABLE II
CER SIMULATION RESULTS

SNR (dB)	CER
11	24%
13	18.3%
15	12.5%
17	9.3%
19	0

TABLE III
BER SIMULATION RESULTS

CER	BER
10%	0.38%
20%	3.1%

TABLE IV
PER SIMULATION RESULTS

BER	PER
3.1%	5.1%
0.38%	0%(< 0.1%)

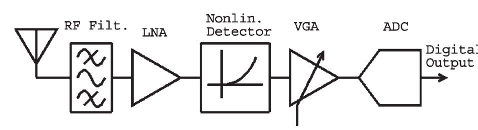

Fig. 14. Downlink-receiver architecture.

PPM-modulated triangular-sinusoid UWB pulse transmissions in MATLAB (which takes about 90 min on an AMD Turion X2 laptop). Under the assumption of 8-b pseudorandom spreading, the CER to bit-error-rate (BER) result is given in Table III. After packet detection and ECC decoding, the BER to packet-error-rate (PER) result is given in Table IV. The PER information will be used in the design of the communication protocol as a measure of the PHY layer performance. Specifically, we design a protocol, as will be discussed in Section VI, under the assumed PER of 5%, since channel measurements show that SNR is around 12 dB for the pulse duration.

B. Downlink Communication

Downlink transmission from PAN coordinator to tire sensor nodes is used primarily to transmit minimal information for MAC scheduling, as detailed in Section VI. Due to the low-data-rate requirements, narrowband communication is used. Furthermore, we apply an ultra-low-power radio design due to power restrictions of the sensor nodes. The power of the downlink receiver needs to be under 100 μW. The only viable architecture to demonstrate this low of a receiver power is based on energy-detection [18]. Other radio receivers have been demonstrated with system powers on the order of a few hundred microwatts. The key to using less than 100 μW is the elimination of the local oscillator and the use of a low-power MEMS-based bulk-acoustic-wave (BAW) front-end filter. This influences most other decisions in the receiver design and yields the basic architecture, as shown in Fig. 14. Its basic operation consists of determining whether RF energy exists in a given frequency band. The signal is coded for interference mitigation.

The operation of the receive chain is as follows. The incoming signal is first filtered so that only the narrowband of interest is admitted. The performance of this BAW filter is

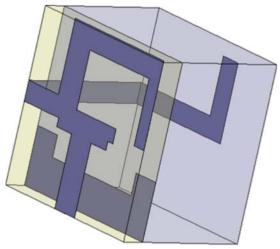

Fig. 15. Example antenna design.

crucial to the operation of the receiver, since any RF energy that is admitted by this filter is detected by the receiver. The MEMS technology also helps in reducing power consumption. The RF signal is then amplified by a low-noise amplifier, which provides a modest gain (10–15 dB) while adding minimal noise. The signal is then demodulated by a nonlinear element. The resulting signal has power at baseband if there is energy at RF. The signal is then low-pass filtered to detect the energy at baseband. The energy is integrated and then digitized. OOK modulation is used, and bit detection uses a single threshold detector on the digitized input stream.

C. Antenna Design

The node requires two antennas: one for the UWB uplink radio and one for the narrowband downlink radio. Efficient antennas are usually on the order of 1/2 of the wavelength of interest in some physical dimension [25]. For example, the length of thin-wire dipole antenna is 1/2 of the wavelength of the center frequency. This presents a problem to the current system, since the node is much smaller than the wavelengths of interest. Furthermore, the antenna is not allowed to stick out from the node, which means that the other parts of the node are part of the near field of the antenna. This could cause the field pattern to change significantly as well as shifting the tuning point of the antenna. The antenna is also restricted to the surface of the node to avoid blocking the antenna's radiation, since the interior of the node will be filled with other subsystems. Moreover, the antenna location is very near metal mesh of the tire, which impacts performance. Note that all of these issues essentially relate to the physical size or extent of the antenna.

There are various techniques to deal with the earlier issues. One way is to reduce the physical size required for a resonant antenna by employing various miniaturization techniques [26] such as substrates with high dielectric constants and slow-wave structures. A related technique simply uses antennas that are less than 1/2 the wavelength (possibly much less) which are not themselves resonant. More complex matching techniques are then used to make these small nonresonant antennas radiate and receive efficiently. The matching requirements tend to be sensitive to changes, including the near-field physical environment for narrowband antennas. In the case of wideband antennas, the matching requirements can be quite difficult to achieve.

Some preliminary designs use more than one face of the node by wrapping the antenna around two or even three sides of the cube (see Fig. 15 for example antenna design). This allows a longer length for the antenna but is much more complex to analyze, requiring numerical simulations. This has the potential to exacerbate the proximity effects of the rest of the node on the antenna, as well as from the other antenna. If both the UWB antenna and the narrowband antenna wrap around multiple sides of the cube, they will become entangled and affect each other's fields. It is advantageous to design a single radiating structure that operates in two bands: the UWB band as well as the ISM band for the narrowband radio. This requires more complex isolation circuitry, but should be possible, since the two radios will not operate at the same time, according to the MAC scheme presented in this paper.

VI. Protocol Design

The MAC protocol manages medium contention between different sensor nodes. A well-designed MAC for wireless applications not only minimizes medium-access contention but also achieves this with minimal energy and delay overhead [24].

MAC protocols can be classified using four main categories: random access, frequency-division multiple access (FDMA), code-division multiple access (CDMA), and time-division multiple access (TDMA) [21]. Due to the relatively large amount of information bits that need to be transmitted within a limited time window in the Intelligent Tire system, random-access schemes, which takes time to assess channel conditions before each transmission, are not suited. FDMA is not a solution, since the needed frequency programmability increases the complexity of the sensor nodes, which results in higher energy consumption and cost. CDMA is a viable choice; however, the harsh channel conditions make intersymbol interference among the sensor nodes a concern. In addition, extra coding may be needed, which reduces the overall throughput of information bits in the system. TDMA has several advantages for our application.

1) It allows nodes to transmit only during the allotted time slot and sleep, otherwise, to save power.
2) During the assigned transmission time, the sensor node will not have to contend with any other sensor for channel access, reducing interference and delay.
3) No extra circuitry is needed; thus, the energy overhead is very low.

On the other hand, TDMA does have shorter transmission time per sensor node as compared with CDMA or FDMA; however, since we only have a maximum of three sensor nodes per tire, this will not present a major problem.

Hence, TDMA seems to be the best choice. However, we cannot use existing schemes [19], [20], which require either a long scheduling instructions from the PAN coordinator or some complex network-synchronization scheme. Due to power limitations, we cannot afford a standard RF receiver on the sensor node. Only limited information can be received via a wake-up radio. Therefore, we must control media access by sending as little information to the sensor nodes as possible. In response to these considerations, we propose a new MAC protocol, which applies to a special class of ultra-low-power data-acquisition wireless networks, where the sensor nodes are subject to stringent energy constraints.

The proposed MAC scheme, called ISTD-MAC, is a TDMA protocol that features implicit generation of a transmission schedule using an ordered-priority scheme. Each node determines its own allocated time-slot based on very limited information sent by the PAN coordinator via the beacon packet.

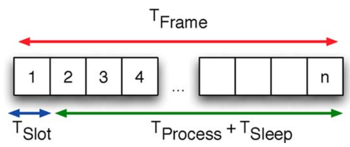

Fig. 16. T_{frame} consists of n T_{slot}, where T_{slot} is the time allotted for a single-sensor node to transmit data and n denotes the number of nodes in the system.

This implicit method simplifies node receiver architecture and energy consumption.

Note that, while ISTD-MAC was expressly developed for the Intelligent Tire system, it can be used in a fairly large set of power-limited WSN applications. For our application, three types of communication activity have to be managed: network initialization, data transmission, and retransmission.

A. Network Initialization

Upon acquiring relevant data from the sensors, a master node initializes network communication by sending a beacon-request packet(s) to the PAN coordinator when the power supply becomes sufficient. The master node repeatedly sends the beacon request packet(s) until a beacon packet is received from the PAN coordinator. Based on the time arrival of the beacon-request packet sent by the master node, the beacon packet carries the following information:

1) the total data-transmission time allocated for the network T_{tx0};
2) the time left for transmission T_{tx};
3) the number of nodes that are currently in the network N.

The beacon is transmitted periodically (every T_{frame}) until the PAN coordinator has received valid packets from all N nodes. With each beacon transmission, the beacon packet is updated with the information of how much more time is left for the current transmission interval T_{tx}. In addition, the PAN coordinator also updates itself for when to generate the appropriate beacon for the next transmission interval. This information is based on its knowledge of the transmission cycles, when the initial beacon request from the master node was received, and possible additional system information.

B. Data Transmission

Upon receiving the beacon packet, the node updates the local T_{tx}, T_{tx0}, and N to implicitly generate the transmit schedule. Each node is associated with an order number a_i, $a_i \in \{1, \ldots, N\}$. Based on a_i and the beacon information, we can determine $T_{\text{wait initial}_i}$ and T_{frame}, which implicitly give us the TDMA schedule of the network

$$T_{\text{wait initial}_i} = a_i * T_{\text{slot}} \quad (2)$$
$$T_{\text{frame}} = N * T_{\text{slot}}. \quad (3)$$

Fig. 16 shows the assumed time-slot structure. Each node waits for $T_{\text{wait initial}_i}$ time until its allocated transmission slot. After the allotted transmission slot has expired, the node goes back into wait mode to prepare for the next transmission slot. A guard time of 0.1 T_{slot} is used between sensor nodes to avoid possible interferences due to clock mismatches. The assignment of T_{slot} and guard time is a tradeoff between transmission fairness, internode interference, and delay overhead. We want to reduce delay overhead by assigning a large T_{slot} to reduce the number of guard intervals and to shrink the duration of the guard intervals; however, we also need to make sure that the guard intervals are long enough to eliminate possible packet collisions between sensor nodes. In addition, we want to maintain a fairness of channel conditions for all the sensor nodes by interleaving transmission such that no sensor node transmits only during good channel conditions or vice versa. Simulation shows that a T_{slot} of ten packet transmissions with 10% guard interval works well for the Intelligent Tire system, but a more rigorous optimization might be needed to further increase system throughput.

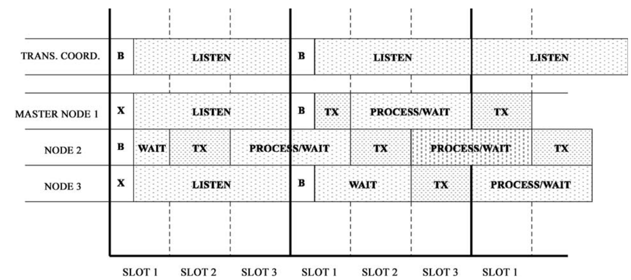

Fig. 17. Transmission schedule of ISTD-MAC for Intelligent Tire system.

The node waits T_{frame} after each transmission slot before transmitting again. This automatic-scheduling mechanism is the heart of our MAC scheme. Each node avoids having to receive complex scheduling instructions explicitly from the PAN coordinator. During the wait periods, the node processes data to prepare for the following transmission frame. Thus, the nodes only perform one function at any given time, lowering the peak energy consumption. The transmission cycle continues until either no more data are available to be sent or the current transmission interval has expired. If there are no data to transmit during the allocated transmission slot, the node sends a keep-alive packet to remain synchronized with the PAN coordinator and goes into sleep mode.

Fig. 17 shows an instance of the transmission schedule for the Intelligent Tire system. In this case, the beacon packet was initially missed by nodes 1 and 2; however, subsequent transmissions were still operational without any medium-access conflicts due to the implicitly generated schedule.

C. Retransmission

ISTD-MAC reduces the PER with a retransmission scheme. During retransmission, the PAN coordinator begins to broadcast R_{beacon} packets during the last 10% of the current transmission cycle. R_{beacon} contains the IDs of all the missing packets from each node. During this time, the nodes also go into listening phase. Upon receiving a complete R_{beacon} packet, the receiver is turned off. If no retransmission is needed, nodes will go into sleep mode. Note that retransmission is explicitly scheduled at the PAN, since we expect only a limited number of retransmissions needed. Thus, R_{beacon} packet will not be a burden for the downlink receiver. All transmission cease at the end of T_{tx0}.

Fig. 18 shows an instance of the retransmission scheme. Note that if the sensor node misses the R_{beacon} packet, then the PAN coordinator continues to request the missing packets at the next

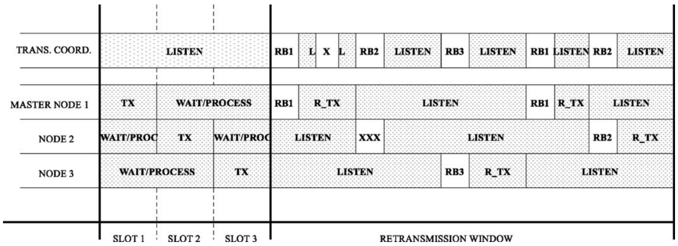

Fig. 18. Retransmission-scheduling scheme.

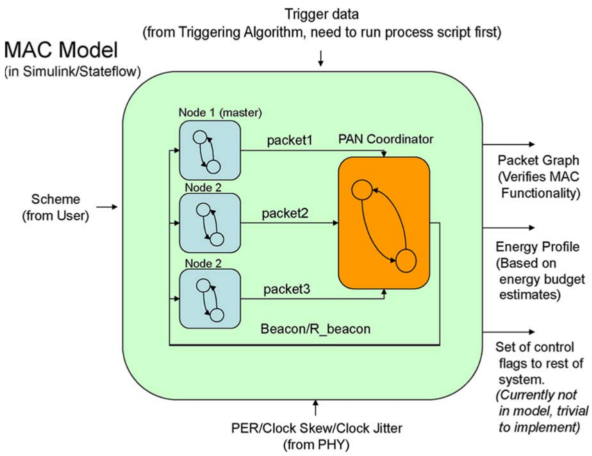

Fig. 19. MAC CFSM model.

retransmission frame, as long as the total transmission time T_{tx0} has not expired.

D. MAC Analysis

To verify the functionality of ISTD-MAC, we created, in Simulink, a codesign finite-state machine (CFSM) [17], which is a globally asynchronous–locally synchronous model of computation. As shown in Fig. 19, the sensor nodes and PAN coordinator are modeled as FSMs, each synchronized to a local clock. Operations in sensor nodes are annotated with estimated energy-consumption figures. To simulate real operation conditions, the communication between sensor nodes and PAN coordinator is modeled as an asynchronous process. Taking input from the triggering algorithm, as well as extracted PHY layer nonidealities such as PER, clock jitter, and clock skew, the MAC model generates a stream of received packets for validation of the protocol and an energy profile for each of the sensor nodes.

Fig. 20 shows the PER performance of the system (i.e., cumulative for all three sensors), with and without packet retransmission as a function of single-sensor PER. The simulation setup assumed 1-Mb/s data rate, 40-B packet size, 10 packet transmissions per allocated time slot per sensor, 18 full wheel rotations with varying velocities, and triggering data from actual sensor data. Without retransmission, the PER of the overall system is roughly the same as the nominal single-sensor PER. No additional packet errors were added to the system; therefore, we can conclude that no medium contentions (i.e., packet collisions) between the sensor nodes occurred. With retransmission, the system PER dropped to well below 1%, with a maximum PER reduction of 95%, simply by allocating 10% of the transmission window for retransmission.

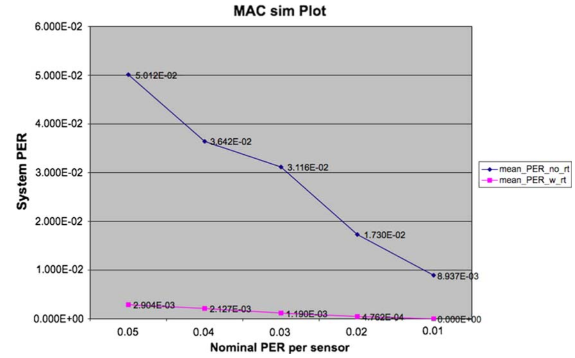

Fig. 20. System PER versus nominal PER plot from MAC simulations.

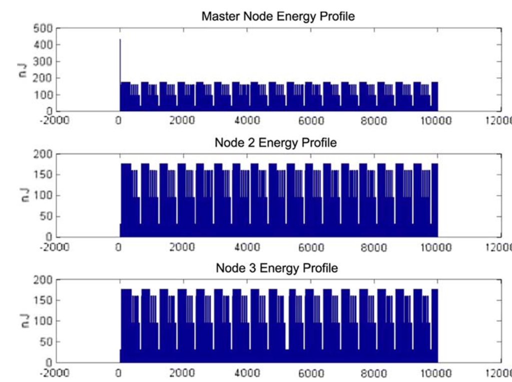

Fig. 21. MAC energy profile for nodes 1, 2, and 3.

Fig. 21 shows the energy profile of the sensor nodes at different intervals of operation. With the exception of network initialization in the master node, energy consumption is kept below 175 nJ per packet time (320 μs) at any given time. This is roughly 55% of the total power available, assuming a 1-mW power source. The rest the energy can be stored for other operations of the sensor node. Although the energy profiles are based on preliminary energy estimation, we can infer that the MAC protocol spreads the sensor operation through time so that the peak power consumption is kept low. Thus, ISTD-MAC is able to virtually eliminate medium contention while still staying within the assumed energy budget of 1 mW.

VII. Design-Space-Exploration Strategy

As discussed previously, the design of the Intelligent Tire system requires expertise in multiple engineering disciplines, including integrated-circuit design, communications, signal processing, real-time software design, antenna design, energy scavenging, and system assembly. In addition, the harsh operating conditions require aggressive design-space exploration, not only for each individual component but also for the system as a whole. The design methodology we adopted is platform-based design (PBD) [27]. The methodology is a meet-in-the-middle process that allows for systematic design-space exploration, where successive refinements of the application specifications meet various abstractions of potential implementations. The orthogonalization of concerns is key to PBD. By separating application functionality from architecture implementation, PBD can be utilized to design very complex heterogeneous systems.

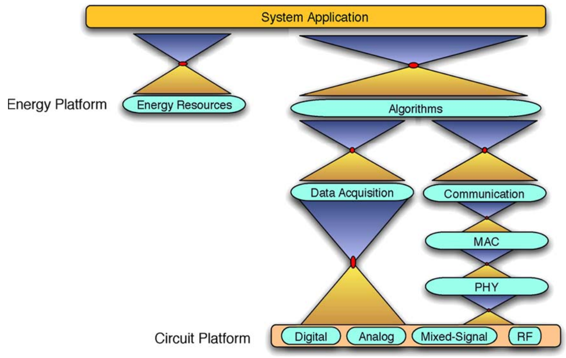

Fig. 22. PBD for Intelligent Tire system.

Currently, there are no commercial PBD-based toolset that can deal with such a heterogeneous system as the Intelligent Tires; however, PBD is still the core strategy used in design-space exploration of this paper. Fig. 22 shows how PBD is applied to the Intelligent Tire system. First, we separate the required functionality of the system from the available energy resources. Note that, although energy resources and the signal-processing algorithms were decoupled, decisions made on the energy platform still impact which implementations are feasible for the application. Thus, an order is needed for design-space exploration. Specifically, we first narrow down the energy resources that suit our application to provide an energy budget. This result is then used as a constraint as we map the system functionality to hardware architecture. The next step in exploration is to map the application onto a set of algorithms, which directly constrain the type of signal acquisition and communication networks needed for the system. We should also note here that even though the communication and data-acquisition functionalities of the system can be represented at the same level of abstraction using, for example, a data-flow model, we still orthogonalize the problem to reduce complexity at lower levels of exploration. The intricacies of the wireless-communication problem require more levels of abstraction for efficient design-space exploration, such as the MAC and the PHY layers of the OSI model, whereas the data-acquisition network can be mapped directly to the circuit platform for physical implementation. The interaction between the MAC and the PHY layers were already mentioned in Sections V and VI. At each level of abstraction, as shown in Fig. 22, we must map the propagated constraints onto a set of components that represent performance abstractions of lower level implementations. Due to the lack of PBD-compliant tools, as well as available libraries, for such a novel application as Intelligent Tires, the mapping process has mostly been manual and simulation based. However, the experiences gained, as well as the models built, will be instrumental in perfecting our methodology and toolset for second-generation implementations of this application or similar ultra-low-power sensor-network applications. In addition to implementation, automatic mapping of data-acquisition and communication schemes onto hardware implementation is currently being explored.

VIII. Conclusion and Future Work

We presented the architecture and the considerations that were used to design a complex wireless sensor network for automotive-safety applications. The wireless sensor network is based on sensor nodes placed inside each tire of an automobile that measure a number of important values to diagnose and control stability and traction. The design of an Intelligent Tire system requires expertise in multiple engineering disciplines including integrated-circuit design, communications, signal processing, real-time software design, antenna design, energy scavenging, and system assembly. In addition, the strict requirements in terms of energy consumption, data rate, delay, and reliability require aggressive design-space exploration, not only for each individual component but also for the system as a whole. A PBD approach was used to deal with the design complexities of this challenging system.

In summary, we first mapped the application onto a set of algorithms, which determines the required resolution and rate of the signal acquisition, and delay and reliability requirements for the communication network. We then determined the best energy source to be batteryless technology based on either energy scavenging or on external power delivery via an RF link. These constraints are then used in mapping the system functionality to hardware architecture. The severe multipath environment of the tire and extreme energy constraints resulted in the choice of impulse-based UWB transmitter and energy-detection receiver at the tire sensor nodes. The issues and tradeoffs in choosing transmitter and receiver architectures were discussed. Moreover, the energy constraints when combined with delay and reliability requirements of the application resulted in a new TDMA-based MAC protocol design.

Several experimental tests have been carried out in Vizzola Ticino Pirelli Track by using different tires at different speeds, different tracks, and different sensor positioning. The measurements show that, depending on the parameter and the relating algorithm involved, a resolution in the range of 11–16 b and a maximum sampling frequency of 10 kHz for each channel is needed to get useful information. In the present configuration, the sensor node may choose to either transmit raw data to the onvehicle PAN coordinator, where postprocessing is carried out to obtain final control quantities such as friction and slip angle, or to process the data directly and transmit the final control quantities to the PAN coordinator at a lower data rate. A correct tradeoff between the amount of processing and transmission of sensor nodes depends on the complexity of the algorithms, the capability of microprocessor on the sensor nodes, and the required parameters from other electronic control units in the vehicle such as steering angle and speed.

We are presently working toward a fully working prototype of the system, and we are researching innovative applications that utilize the underlying technology. To aid in realizing the prototype, we will focus our design methodology on mixed-signal systems. We will focus on populating the general PBD framework with a set of tools and methods to support the following features:

1) efficient and accurate modeling of circuit (RF, analog, digital, and mixed signal) performance space to create a comprehensive component library to serve as a platform for high-level system design;
2) automatic physical architecture synthesis (component composition) of mixed-signal systems given application-specific signal-processing algorithms and the component library to generate the set of all feasible architectures;

3) global (architecture and circuit configuration) system optimization to determine optimal system design for the given application.

These tools and methods will help in determining to best mapping of the Intelligent Tire system's signal acquisition and communication functionalities onto the set of available circuit components to minimize overall system cost.

REFERENCES

[1] T. Schrüllkamp, H. Goertz, and T. Hüsemann, "Development of an intelligent tire—Experiences from the APOLLO project," in *Intell. Tire Technol. Conf.*, Frankfurt, Germany, Nov. 2005.

[2] J. Yi, "A piezo-sensor-based 'smart tire' system for mobile robots and vehicles," *IEEE/ASME Trans. Mechatronics*, vol. 13, no. 1, pp. 95–103, Feb. 2008.

[3] A. Todoroki, S. Miyatani, and Y. Shimamura, "Wireless strain monitoring using electrical capacitance change of tire with oscillating circuit," *Smart Mater. Struct.*, vol. 12, no. 3, pp. 403–409, Jun. 2003.

[4] N. Robinson, III and J. H. Matthews, "Remote tire pressure monitoring system employing coded tire identification and radio frequency transmission and enabling recalibration upon tire rotation or replacement," Patent: 5 838 229, Nov. 17, 1998.

[5] K. E. Mattson, L. W. Hamm, W. K. Cotton, R. A. Stewart, M. A. Uleski, R. B. Belden, and M. A. Peterson, "Tire pressure monitor system with side entry pressure port," Patent: 7 377 156, May 27, 2008.

[6] J. P. Robillard, B. S. Honeck, J. R. Geschke, and M. J. Suman, "Tire monitoring system," Patent: 6 259 361, Jul. 10, 2001.

[7] R. Behringer and N. Muller, "Autonomous road vehicle guidance from autobahnen to narrow curves," *IEEE Trans. Robot. Autom.*, vol. 14, no. 5, pp. 810–815, Oct. 1998.

[8] A. Nepote, P. Pierre, T. Varpula, A. Rautiainen, and K. Jaakkola, "The intelligent tire: Acceleration sensors data acquisition," in *SAE World Congr.*, Apr. 2005, pp. 59–66.

[9] World Health Organization, *World Report on Road Traffic Injury Prevention*, 2004.

[10] S. Muller, M. Uchanski, and K. Hedrick, "Estimation of the maximum tire–road friction coefficient," *Trans. ASME, J. Dyn. Syst. Meas. Control*, vol. 125, no. 4, pp. 607–617, Dec. 2003.

[11] F. Gustafsson, "Slip-based tire–road friction estimation," *Automatica*, vol. 33, no. 6, pp. 1087–1099, Jun. 1997.

[12] A. F. Molisch, K. Balakrishnan, D. Cassioli, C.-C. Chong, S. Emami, A. Fort, J. Karedal, J. Kunisch, H. Schantz, and K. Siwiak, "A comprehensive model for ultrawideband propagation channels," in IEEE GLOBECOM, Nov. 2005, vol. 6, pp. 3648–3653.

[13] *IEEE 802.15.TG4a Official Web Page*. [Online]. Available: http://www.ieee801.org/15/pub/tg4a.html

[14] H. Sheng, P. Orlik, A. Haimovich, L. C. Cimini, Jr., and J. Zhang, "On the spectral and power requirements for ultra-wideband transmission," in *IEEE Int. Conf. Commun*, 2003, pp. 738–742.

[15] V. Somayazulu, J. R. Forester, and S. Roy, "Design challenges for very high data rate UWB systems," in *Conf. Rec. 36th Asilomar Conf. Signals, Syst., Comput.*, Nov. 2002, vol. 1, pp. 717–721.

[16] X. Shen, M. Guizani, R. Qiu, and T. Le-Ngoc, *Ultra-Wideband Wireless Communications and Networks*. Hoboken, NJ: Wiley, 2006.

[17] F. Balarin, H. Hseih, A. Jurecska, L. Lavagno, and A. Sangiovanni-Vincentelli, "Formal verification of embedded systems based on CFSM networks," in *Proc. 33rd Annu. Conf. Des. Autom.*, 1996, pp. 568–571.

[18] N. Pletcher, S. Gambini, and J. Rabaey, "A 65 uW, 1.9 GHz RF to digital baseband wakeup receiver for wireless sensor nodes," in *Proc. Custom Integr. Circuits Conf.*, San Jose, CA, Sep. 2007, pp. 539–542.

[19] D. Networks, *Technical Overview of Time Synchronized Mesh Protocol (TSMP)*, Jun. 2006. document number: 025-0003-01.

[20] S. Coleri and P. Varaiya, "PEDAMACS: Power efficient and delay aware medium access protocol for sensor networks," *IEEE Trans. Mobile Comput.*, vol. 5, no. 7, pp. 920–930, Jul. 2006.

[21] J. G. Proakis, *Digital Communications*, 4th ed. New York: McGraw-Hill, 2001.

[22] A. Goldsmith, *Wireless Communications*. Cambridge, U.K.: Cambridge Univ. Press, 2005.

[23] A. V. Oppenheim and R. W. Schafer, *Discrete-Time Signal Processing*. Englewood Cliffs, NJ: Prentice-Hall, 1999.

[24] M. G. D. Benedetto and G. Giancola, *Understanding Ultra Wide Band Radio Fundamentals*. Englewood Cliffs, NJ: Prentice-Hall, 2004.

[25] C. Balanis, *Antenna Theory: Analysis and Design*, 3rd ed. Hoboken, NJ: Wiley, 2005.

[26] P. Bhartia, I. Bahl, R. Garg, and A. Ittipiboon, *Microstrip Antenna Design Handbook*. Norwood, MA: Artech House, 2000.

[27] A. Sangiovanni-Vincentelli, L. Carloni, F. D. Bernardinis, and M. Sgroi, "Benefits and challenges for platform-based design," in *Proc. 41st Annu. DAC*, 2004, pp. 409–414.

[28] S. Roundy, M. Strasser, and P. K. Wright, *Powering Ambient Intelligent Networks*. Berlin, Germany: Springer-Verlag, Dec. 2005, pp. 271–299.

Sinem Coleri Ergen (S'98–M'07) received the B.S. degree in electrical and electronics engineering from Bilkent University, Ankara, Turkey, in 2000 and the M.S. and Ph.D. degrees in electrical engineering and computer sciences from the University of California, Berkeley, Berkeley, in 2002 and 2005, respectively.

Since July 2006, she has been a Research Scientist with the Wireless Sensor Networks Berkeley Laboratory, Berkeley, which is under the sponsorship of Pirelli and Telecom Italia. Her research interests include wireless communications and networking, collaborative signal processing, and embedded systems.

Dr. Ergen was the recipient of the Regents Fellowship from the University of California, Berkeley, in 2000, and the Bilkent University Full Scholarship from Bilkent University in 1995.

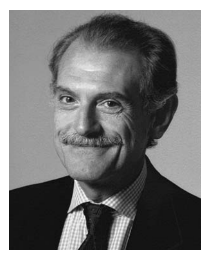

Alberto Sangiovanni-Vincentelli (F'82) received the "Dottore in Ingegneria" degree (*summa cum laude*) in electrical engineering and computer science from the Politecnico di Milano, Milano, Italy, in 1971.

From 1980 to 1981, he was a Visiting Scientist in the Mathematical Sciences Department, IBM T. J. Watson Research Center, Yorktown Heights, NY. In 1987, he was a Visiting Professor at Massachusetts Institute of Technology, Cambridge. He has held a number of Visiting Professor positions at Italian Universities, including Politecnico di Torino, Torino, Italy; Universita' di Roma, La Sapienza, Rome, Italy; Universita' di Roma, Tor Vergata, Rome; Universita' di Pavia, Pavia, Italy; and Universita' di Pisa, Scuola di Sant'Anna, Pisa, Italy. He was a cofounder of Cadence and Synopsys, the two leading companies in the area of electronic design automation. He is currently the Chief Technology Adviser of Cadence. He is a member of the Board of Directors of Cadence and the Chair of its Technology Committee, UPEK, a company he helped spinning off from ST Microelectronics, Sonics, and Accent, an ST Microelectronics–Cadence joint venture he helped founding. He was a member of the HP Strategic Technology Advisory Board. He is currently a member of the Science and Technology Advisory Board of General Motors and of the Scientific Council of the Tronchetti Provera Foundation and of the Snaidero Foundation. He is currently the Edgar L. and Harold H. Buttner Chair of Electrical Engineering and Computer Sciences with the Department of Electrical Engineering and Computer Science, University of California, Berkeley, Berkeley, where he has been on the faculty since 1976. He consulted for many companies including Bell Laboratories, IBM, Intel, United Technologies Corporation, COMAU, Magneti Marelli, Pirelli, BMW, Daimler–Chrysler, Fujitsu, Kawasaki Steel, Sony, ST, United Technologies Corporation, and Hitachi. He was an Advisor to the Singapore Government for microelectronics and new ventures. He consulted for Greylock Ventures and for Vertex Investment Venture Capital funds. He is a member of the Advisory Board of Walden International, Sofinnova, and Innogest Venture Capital Funds and a member of the Investment Committee of a novel VC Fund, Atlante Ventures, by Banca Intesa/San Paolo. He is the founder and Scientific Director of the Project on Advanced Research on Architectures and Design of Electronic Systems, a European Group of Economic Interest supported by Cadence, Magneti–Marelli, and ST Microelectronics. He is a member of the Advisory Board of the Lester Center for Innovation of the Haas School of Business and of the Center for Western European Studies and is a member of the Berkeley Roundtable of the International Economy. He is a member of the High-Level Group, of the Steering Committee, of the Governing Board, and of the Public Authorities Board of the EU Artemis Joint Technology Initiative. He is a member of the Scientific Council of the Italian National Science Foundation. He is an author of over 800 papers, 15 books, and 3 patents in the area of design tools and methodologies, large-scale systems, embedded systems, hybrid systems, and innovation.

Prof. Sangiovanni-Vincentelli was the recipient of the Distinguished Teaching Award of the University of California in 1981. He was also the recipient of the worldwide 1995 Graduate Teaching Award of the IEEE (a Technical Field Award for "inspirational teaching of graduate students"). In 2002, he was the recipient of the Aristotle Award of the Semiconductor Research Corporation. He was the recipient of numerous research awards, including the Guillemin–Cauer Award (1982–1983), the Darlington Award (1987–1988) of the IEEE for the best paper bridging theory and applications, and two awards for the best paper published in the IEEE TRANSACTIONS ON CIRCUITS AND SYSTEMS and IEEE TRANSACTIONS ON COMPUTER-AIDED DESIGN OF INTEGRATED CIRCUITS AND SYSTEMS. He was also the recipient of five best paper awards and one best presentation awards at the Design Automation Conference and other best paper awards at the Real-Time Systems Symposium and the VLSI Conference. In 2001, he was the recipient of the Kaufman Award of the Electronic Design Automation Council for "pioneering contributions to EDA." In 2008, he was the recipient of the IEEE/RSE Wolfson James Clerk Maxwell Medal "for groundbreaking contributions that have had an exceptional impact on the development of electronics and electrical engineering or related fields" with the following citation: "For pioneering innovation and leadership in electronic design automation that have enabled the design of modern electronics systems and their industrial implementation." He is a member of the National Academy of Engineering, which is the highest honor bestowed upon a U.S. Engineer, since 1998.

Xuening Sun (M'02) received the B.S.E.E. degree (with highest honors) from the University of Texas at Austin, Austin, in 2004 and the M.S. degree from the University of California, Berkeley, Berkeley, in 2007, where he is currently working toward the Ph.D. degree in the Department of Electrical Engineering and Computer Science.

In 2005, he was with IBM, Austin, where he was a Design Engineer for the zSeries server processor family before pursuing graduate studies in electronic design automation. In the summers of 2006 and 2007, he was a Research Intern at the Pirelli/Telecom Italia Wireless Sensor Networks Laboratory, Berkeley, where he was involved in ultrawideband system modeling and MAC protocol design. His research interests include electronic-system-level design methodologies, with a special interest in system-level composition of analog/RF circuits.

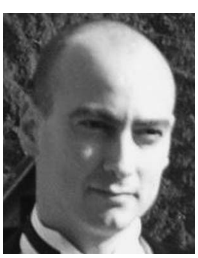

Riccardo Tebano received the Laurea degree in physics from the Università degli Studi di Milano, Milano, Italy, in 1998 and the Ph.D. degree from the Università degli Studi di Milano-Bicocca, Milano, in 2001.

He is currently with the Tyre System and Vehicle Dynamics Department, Pirelli Tyre S.p.A., Milano, Italy.

Sayf Alalusi received the B.S., M.S., and Ph.D. degrees from the University of California, Berkeley, in 1998, 2001, and 2005, respectively.

He first worked for HRL Laboratories Malibu, CA, on many diverse research tasks. He then joined the Wireless Sensor Networks Berkeley Laboratory, Berkeley, where he worked on low-power radios and wireless energy transfer projects for Pirelli's Smart Tire initiative. He is currently with TransRobotics, an early-stage start-up company in the San Francisco Bay Area, Hayward, CA, specializing in industrial sensing and automation.

Giorgio Audisio received the degree in electrical engineering from the Politecnico di Torino, Torino, Italy, in 1985.

He started his professional career with the Telecom Research Institute. In 1987, he joined Fiat Auto, where he was appointed Head of the Electrical and Electronic Design Centre in 1997. During these years, his team redesigned all the electrical and electronic architectures of Fiat, Alfa, and Lancia models with a dramatic improvement of reliability and cost reduction. After a period as Director of Innovation, he was appointed as Deputy Director of the Electrical and Electronic Competence Area, where he led the joint project with Microsoft for the development of a new telematics platform (Blue&Me) which is now deployed in all Fiat Auto and Iveco vehicles. In 2005, he joined Pirelli Tyres S.p.A., Milano, Italy, as Chief Engineer of the Tyre Systems and Vehicle Dynamics Department to lead strategic development projects to transform the tire into an active and "intelligent" tire ("Cyber Tyre").

Marco Sabatini received the Laurea degree (with honors) in electrical engineering from the Politecnico di Milano, Milano, Italy, in 1991.

He was with ST Microelectronics Central R&D, Agrate, Italy, where he worked on innovative HW architecture design. In 1996, he was invited as Visiting Industrial Fellow at the University of California, Berkeley, Berkeley, where he worked on low-power analog-to-digital converter. In 1997, he joined ST Berkeley Laboratories, where he developed advanced CMOS camera and solid state fingerprint-sensor technologies. In 2001, he was appointed as Vice President of Engineering at Barcelona Design, where he was working on automatic synthesis of analog-circuit topologies. In 2004, he returns to Italy and worked at Accent S.r.l. in the design and consulting service in the wireless-sensor field. In 2008, he joined Pirelli Tyres S.p.A., Milano, where he is currently responsible for technologies for the "Cyber Tyre" project. He has published more than 17 patents and 7 papers at International Electron Devices Meeting, International Solid State Circuits Conference (ISSCC), and other conferences. He was also assigned an "Exceptional Patent Award" by ST Microelectronics in 2000.